

# Modeling Drug Transport Through the Blood–Brain Barrier

Touss Majidi, Robert Picardo, Vageeshwar Srinivasan, and Stephanus Yang

*BIOENG 104: Biological Transport Phenomena, Spring 2024*

*Department of Bioengineering, University of California, Berkeley, CA*

**Abstract**—Alzheimer’s disease (AD) is a neurodegenerative condition that leads to symptoms of memory loss and dementia. Although these symptoms can be treated with effective drug administration, the actual efficacy of these treatments is reduced profoundly by the low permeability of the blood–brain barrier (BBB). The BBB is a semipermeable, multilayered membrane that serves as the interface and key molecule transporter between the cardiovascular and central nervous systems. It is of great interest to examine the effects of deterioration on the BBB, induced by AD progression, on drug delivery.

In the present paper, we carry out a sensitivity analysis examining the effects of porosity of the BBB onto the concentration profile and transport mechanism of donepezil, a commonly used AD drug, through the multilayered barrier and into brain tissue. A numerical study was generated, recreating the BBB between the capillary domain and brain tissue region. Using governing equations of convective and diffusive transport, we investigated the spatiotemporal concentration profiles of donepezil and the Péclet number under various porosities. Our results show that at increased porosities, the drug concentration profile is also amplified, leading to increased drug delivery efficacy. From the Péclet number, a sharp progression from convective to diffusive dominating transport was found from the capillary domain to the BBB and brain parenchyma. Additionally, increasing porosity slightly promotes convection within the BBB and brain tissue. Despite geometric simplification, our study aims to aid in understanding how deterioration affects drug transport kinetics. This provides insight for the development of more effective therapeutic strategies.

## I. INTRODUCTION

As of 2020, Alzheimer’s disease (AD), the prevailing cause of dementia, affects approximately 50 million patients worldwide; this number is projected to increase up to 152 million by 2050 [1]. A prevailing “cholinergic” hypothesis proposes that AD coincides with reduced biosynthesis of acetylcholine (ACh) due to degeneration of cholinergic neurons [1]. As a result, reduced ACh levels cause alterations in cognitive function. One common therapeutic strategy is to inhibit hydrolytic degradation of ACh in the synaptic cleft. Decreasing the activity of acetylcholinesterase (AChE) inhibitors thereby leads to restorative accumulation of ACh [1], [2] and thus improvement in cognitive function. Several AChE inhibitors, such as galantamine, rivastigmine, and donepezil, are currently used drugs for symptomatic treatment of AD [3], [4]. Therefore, a compelling interest is to optimize transport of AChE inhibitor toward the visceral tissue (or parenchyma) of the brain where the neurons reside.

A major challenge to optimizing non-invasive drug treatment is the drastic reduction in drug transport through the

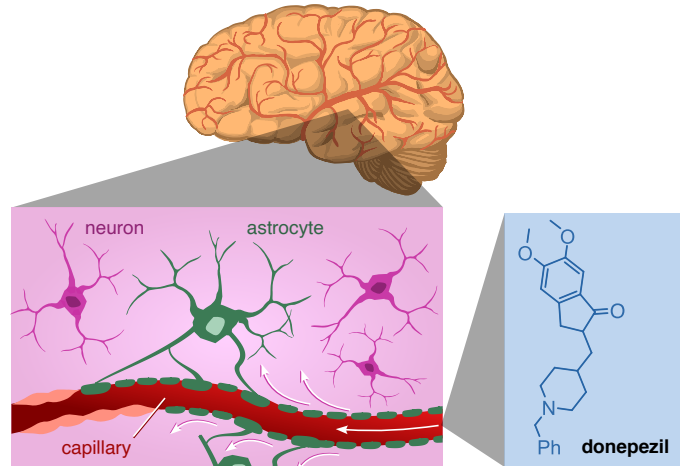


Fig. 1. A general schematic of the location of the blood–brain barrier (BBB) within the brain. Transport of donepezil, an acetylcholinesterase inhibitor, from the capillary domain through the BBB is the main phenomenon modeled by our computational study.

blood–brain barrier (BBB). The BBB, which serves as the interface between the cardiovascular system and the central nervous system (CNS), is a key regulator of ionic, molecular, and cellular transport between blood and brain [5]. The BBB is a multicellular semipermeable membrane essentially composed of endothelial cells, astroglia (fig. 1), pericytes, and junctional complexes [6]. The high degree of impermeability within the membrane is due to the tight and adherens junctions between endothelial cells, which restricts small-molecule drugs from penetrating the BBB via paracellular transport [7].

Two previous studies, namely Hassanzadeganroudsari *et al.* [8] and Sarafraz *et al.* [9], have constructed numerical models of the BBB as a series of membranes in a simplified, axisymmetric geometry. Each of the two studies explored the transport mechanisms of a select therapeutic agent—nanoparticles and transferrin receptor-targeted aptamers, respectively—through the BBB. However, these studies do not leverage their model to explore transport mechanisms of small-molecule drugs, nor do they provide insight on the relation between drug transport and the degree of deterioration of the BBB.

To explore the effects of degradation of the BBB toward drug transport efficacy, we present a sensitivity analysis examining the effects of porosity on simulated transport of donepezil, an effective AchE inhibitor, using a numerical model of the BBB as derived from Sarafraz *et al.* [9]. This

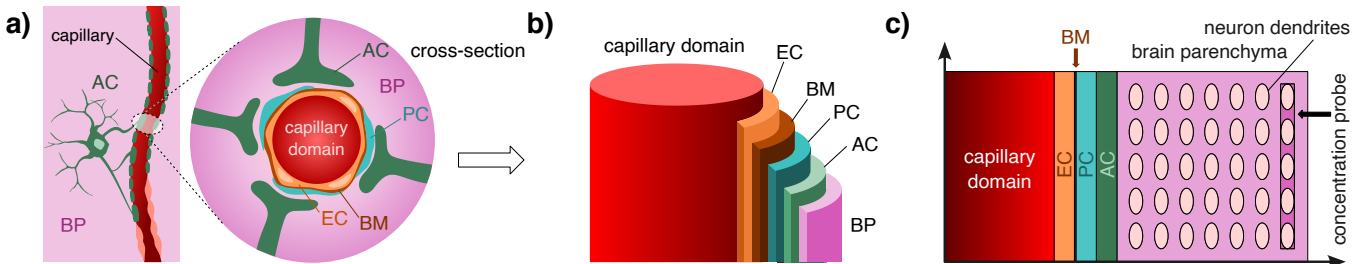


Fig. 2. **a)** A cross-sectional diagram of the capillary domain surrounded by brain parenchyma (BP) and the blood–brain barrier (BBB), with individual layers shown: the endothelial cell (EC) layer, the basement membrane (BM), the pericyte (PC) layer, and the astrocyte (AC) endfeet. **b)** A schematic of the simplified cylindrical geometry of the capillary–BBB–BP domain. **c)** The primary schematic of the 2D axisymmetric model constructed in COMSOL Multiphysics. The concentration probe measures the concentration profile of donepezil over the interdendrite region (dark purple).

model is composed of a series of membranes representing the critical components of the BBB, namely the endothelial cells, basement membrane, pericytes, and the astrocyte endfoot. Additionally, using the governing equations describing diffusive and convective transport, we used this model to explore the effects of porosity on the concentration profiles and the dominating transport mechanism of donepezil.

The outcomes of our study aim to provide a greater understanding on how alterations of the neurophysiological state due to AD can help determine the efficacy of small-molecule drug administration from the cardiovascular system to the CNS.

## II. METHODS

### A. Design and Construction of Numerical Model

To obtain an approximation for the mass transport through the BBB, a computational fluid dynamics simulation was constructed to model the BBB as a multilayered interface between the bloodstream, or capillary domain, and the brain parenchyma. The geometry of the BBB was created using the COMSOL Multiphysics software (version 6.2), over which the governing equations outlining mass transport behaviors were applied and solved via finite element method (FEM) analysis.

Basing our geometry on the previous numerical model by Sarafraz *et al.* [9] as a key reference, our simulation was constructed as a two-dimensional axisymmetric model over cylindrical coordinates  $(r, \theta, z)$ , using the geometric parameters listed in table I. The center of the capillary was assigned as the axis of revolution, and the brain parenchyma was assigned as the region most radially outward from the axis of revolution. Using the thicknesses listed in table I, the BBB was created as a series of porous media, consisting of the endothelial cell layer, the basement membrane, the pericytes, and the astroglial layer (listed in order of increasing  $r$ ).

Lastly, the brain parenchymal region was populated with an array of neuron dendrites ( $7 \times 5$  in the  $r$  and  $z$  directions; fig. 2c). Like in Sarafraz *et al.* [9], the neuron dendrites were assumed to be ovular cross-sections through which there would be no fluid transport.

Furthermore, we outlined a rectangular region, spanning from the top of the uppermost dendrite to the bottom of the bottommost dendrite, with a width equivalent to  $r_N$ . This region encompasses the last column of dendrites to serve as a concentration probe that measures the concentration profile

of donepezil over the interdendrite region, as seen in fig. 2c. Additionally, we embedded a secondary “centerline” probe (fig. 5a) to measure the concentration profile at a fixed  $z$ -position ( $z = 6.2 \mu\text{m}$ ).

We made the following assumptions to our mathematical model:

- 1) *The flow of blood inside the capillary domain is assumed to be laminar and incompressible.* The Reynolds number of blood flow can be described as  $Re = \rho_b u_b L / \mu_b$ , for blood velocity  $u_b$ , blood viscosity  $\mu_b$ , and characteristic length  $L$ , which we assign to be the diameter of the capillary domain. Using the fluid flow parameters listed in table II, the resulting value of  $Re \approx 0.0007 \ll 2000$  corroborates with our assumption of laminar flow.
- 2) *Blood is assumed to behave as a Carreau fluid.* As we aimed to account for its non-Newtonian, shear-thinning properties, we assumed that its flow conforms to the Carreau blood flow model outlined in eq. (4).
- 3) *Donepezil is modeled to have an inlet concentration rather than a fixed concentration throughout the capillary* to mimic *in vivo* conditions (i.e., continuous delivery to the bloodstream from external sources, such as oral administration or intravenous infusion).
- 4) *We assume that mass transport of blood and donepezil is driven by both convection and diffusion throughout the entire domain.*
- 5) *All layers of the BBB are assumed to have equal porosities,* as these porosities are yet to be investigated experimentally [9]. This assumption is primarily for the sake of simplicity and sensitivity analysis.
- 6) *Donepezil is assumed to not react with any biological component in the system.* This assumption was made to reduce computational costs.
- 7) *The flow of blood is fully-developed within the capillary domain.* Since the length of our capillary is extremely minuscule, we have also assumed that the pressure gradient across the capillary is negligible. Likewise, the pressure gradient across the brain parenchyma is negligible.
- 8) *All outside body forces, including gravitational and electric forces, are negligible.* This follows the same rationale as the previous assumption (6).

Finally, like Sarafraz *et al.* [9], we carried on the following conceptual assumptions:

TABLE I  
GEOMETRIC PARAMETERS USED IN NUMERICAL MODEL

Parameter	Value	Unit	Ref.
Thickness of blood capillary ( $r_{\text{cap}}$ )	8	μm	[12]
Thickness of EC layer ( $r_{\text{EC}}$ )	1.5	μm	[13]
Thickness of BM layer ( $r_{\text{BM}}$ )	0.1	μm	[14]
Thickness of pericyte layer ( $r_{\text{PC}}$ )	1.5	μm	[13]
Thickness of astrocyte endfoot ( $r_{\text{AC}}$ )	1.5	μm	[15]
Thickness of brain parenchyma ( $r_p$ )	14	μm	[9]
Length of BBB model ( $z_{\text{model}}$ )	15	μm	[9]
Large diameter of neuron ( $z_N$ )	1	μm	[9]
Small diameter of neuron ( $r_N$ )	0.5	μm	[9]
Approximate diameter of donepezil	0.70	nm	[16]

- 8) *The BBB, as well as mass transport through it, can be approximated as a 2D axisymmetric geometry.* This is the key assumption that reduces computational cost and burden, making our model somewhat versatile. In making this assumption, however, we leave out significant variations in microvasculature, which would greatly affect mass transport profiles.
- 9) *Porosity is the main indicator of the degree of deterioration of the BBB.* It is shown that, due to AD and age-related factors, loosening of the tight junctions between endothelial cells occurs [10]. Additionally, evidence suggests that the penetration of donepezil through the BBB is mediated by carrier-mediated transport [11]. Therefore, we have selected porosity as our main independent parameter because of this tight junction-loosening phenomenon and that carrier-mediated transport is associated with the opening and closing of membrane protein pores.

### B. Governing Equations of Fluid and Drug Transport

1) *Transport of blood flow:* First, a “laminar flow” module was applied to the capillary domain. The capillary domain ( $0 \leq r < r_{\text{cap}}$  and  $0 \leq z \leq z_{\text{model}}$ ), the Navier–Stokes equations, eq. (1), and continuity equation, eq. (2), were solved via FEM analysis to account for the laminar, incompressible flow of blood along time  $t$ :

$$\rho_b \frac{\partial \mathbf{u}}{\partial t} + \rho_b (\mathbf{u} \cdot \nabla) \mathbf{u} = -\nabla p + \nabla \cdot \boldsymbol{\tau} + \rho_b \mathbf{f} \quad (1)$$

$$\frac{\partial \rho_b}{\partial t} + \nabla \cdot (\rho_b \mathbf{u}) = \nabla \cdot (\rho_b \mathbf{u}) = 0 \quad (2)$$

where  $\mathbf{u}$  is the velocity field of donepezil within the blood,  $\rho_b$  the blood density,  $\nabla p$  the pressure gradient, and  $\mathbf{f}$  any body force applied to the fluid. As blood is assumed to be incompressible, the quantity  $\partial \rho_b / \partial t$  contained in eq. (2) is consequently zero. Additionally, our negligible body force assumption renders  $\mathbf{f} \approx \mathbf{0}$ . The stress tensor  $\boldsymbol{\tau}$  can be expressed in terms of blood viscosity and the gradient of its velocity by the constitutive relation

$$\boldsymbol{\tau} = \mu(\dot{\gamma}) [\nabla \mathbf{u} + (\nabla \mathbf{u})^T] \quad (3)$$

where  $\mu(\dot{\gamma})$  is the viscosity of blood, dependent on the shear rate  $\dot{\gamma}$ . From our assumption, blood acts as a shear-thinning fluid and conforms to the Carreau model of blood flow [17]:

$$\mu(\dot{\gamma}) = \mu_\infty + (\mu_0 - \mu_\infty) [1 + (\lambda \dot{\gamma})^2]^{\frac{n-1}{2}} \quad (4)$$

where  $\mu_0$  is the zero shear rate viscosity,  $\mu_\infty$  is the infinite shear rate viscosity,  $\lambda$  is the relaxation time, and  $n$  is the power index. All aforementioned quantities are displayed in table II. Furthermore, the quantity  $\dot{\gamma}$  is the shear rate, determined by the equation

$$\dot{\gamma} = \sqrt{2 \mathbf{S} : \mathbf{S}} \quad (5)$$

for rate-of-strain tensor  $\mathbf{S}$  and the double dot product operator  $(:) \cdot$ . By definition, the rate-of-strain tensor is related to the stress tensor  $\boldsymbol{\tau}$  via

$$\mathbf{S} = \frac{1}{2} [\nabla \mathbf{u} + (\nabla \mathbf{u})^T] \iff \boldsymbol{\tau} = 2\mu \mathbf{S} \quad (6)$$

For the blood–brain barrier ( $r_{\text{cap}} \leq r \leq \sum r_i$  for  $i = \text{cap}, \text{EC}, \text{BM}, \text{PC}, \text{AC}$ ), a “porous medium” module was implemented with Darcian flow. The governing equations describing porous blood flow throughout the BBB due to Darcian flow (eqs. (7) to (9)) were solved for via FEM analysis:

$$\begin{aligned} \frac{\rho}{\varepsilon_p} \frac{\partial \mathbf{u}}{\partial t} + \frac{\rho^2}{\varepsilon_p^2} (\mathbf{u} \cdot \nabla) \mathbf{u} \\ = \nabla \cdot (-p \mathbf{I} + \boldsymbol{\tau}_{\text{por}}) - \left( \mu \kappa^{-1} + \beta \rho \|\mathbf{u}\| + \frac{\rho \nabla \cdot \mathbf{u}}{\varepsilon_p^2} \right) \end{aligned} \quad (7)$$

where the stress tensor through the porous medium can be determined via

$$\boldsymbol{\tau}_{\text{por}} = \frac{\mu}{\varepsilon_p} [\nabla \mathbf{u} + (\nabla \mathbf{u})^T] - \frac{2}{3} \frac{\mu}{\varepsilon_p} (\nabla \cdot \mathbf{u}) \mathbf{I} \quad (8)$$

$$\kappa = \frac{d_p^2}{180} \frac{\varepsilon_p^3}{(1 - \varepsilon_p)^2} \quad (9)$$

Note that  $\mathbf{I}$  is the identity tensor,  $\kappa$  is the permeability of the BBB, and  $d_p$  is the effective diameter of one donepezil molecule (table II). The calculation for permeability  $\kappa$  (eq. (9)) is based on the Kozeny–Carman permeability model [18].

2) *Transport of donepezil:* In the domain outside the capillary, namely the BBB and brain parenchyma, a variant of the advection–diffusion equation for porous media [19] was used as the governing equation:

$$\varepsilon_p \frac{\partial c_i}{\partial t} + \frac{\partial (\rho c_{p,j})}{\partial t} + \nabla \cdot \mathbf{J}_i + \mathbf{u} \cdot \nabla c_i = R_i + S_i \quad (10)$$

where  $c_i = c_i(r, z, t)$  is the concentration profile of donepezil throughout the system, and  $R_i$  and  $S_i$  are the reaction rates. From our assumptions, these reaction rates are declared to be zero. The flux of fluid through the porous media can be obtained by a variant of Fick’s first law:

$$\mathbf{J}_i = -(D_{d,j} + D_{e,j}) \nabla c_i \quad (11)$$

The effective diffusivity  $D_{e,j}$  is calculated

$$D_{e,i} = \frac{\varepsilon_p}{\tau_{F,i}} D_{F,i} \quad (12)$$

given the fluid diffusion coefficient  $D_{F,i}$ , porosity of the medium  $\varepsilon_p$ , and quantity  $\tau_{F,i} = \varepsilon_p^{1/3}$  as predicted by the Millington–Quirk effective diffusivity model.

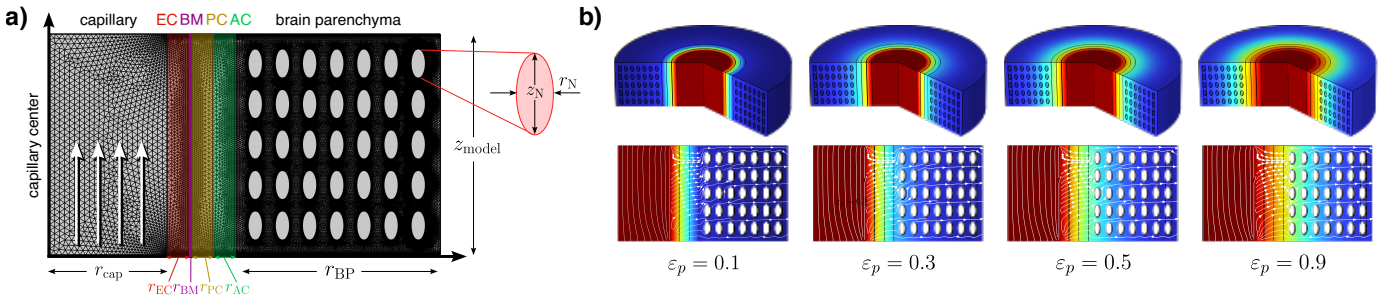


Fig. 3. a) A mesh render of the main numerical model. The total mesh number is 106576 elements (“extra fine”). The total simulation time for the parametric sweep is  $\sim 14$  min. EC = endothelial cell layer; BM = basement membrane; PC = pericyte layer; AC = astrocyte layer. b) The concentration profile (colored) and velocity field (white) on the 2D axisymmetric variant and 3D revolved version of the numerical model for various porosities ( $\varepsilon_p = 0.1, 0.3, 0.5, 0.9$ ) at time  $t = 10$  seconds.

### C. Boundary and Initial Conditions

In our numerical model, we implemented the following critical boundary and initial conditions for our “laminar” blood flow module:

- 1) For the capillary domain (i.e. for all  $z = 0$  and  $0 \leq r \leq r_{\text{cap}}$ ), we assigned an inlet velocity field with magnitude  $u_{b,\text{in}} = 0.38 \text{ mm s}^{-1}$  oriented upstream the vessel.
- 2) Everywhere outside the capillary domain in the porous regimes, the velocity field is initially zero (at  $t = 0$  seconds).
- 3) An outlet boundary condition was assigned at  $z_{\text{model}} = 15 \mu\text{m}$  and at  $0 \leq r \leq r_{\text{cap}}$ . This boundary condition enforced fully-developed flow throughout the capillary domain, despite the assumption of zero pressure gradient driving the flow upwards.
- 4) The interface between the capillary and BBB, at  $r = r_{\text{cap}}$ , was assumed to have a no-slip condition. Additionally, a “porous interface” module was implemented to account for sudden jumps in porosity between the two critical regions.

In our “transport of diluted species” module, we implemented the following boundary and initial conditions:

- 5) An inlet concentration of  $c_{\text{in}} = 1.41 \times 10^{-4} \text{ mol m}^{-3}$ , equivalent to a 5 mg oral dosage of donepezil, was established at the lower segment of the capillary domain ( $z = 0, 0 \leq r \leq r_{\text{cap}}$ ). The motivation behind this value is outlined in section II-D.
- 6) An outflow boundary condition was also established at the farthest wall of the brain parenchyma.
- 7) The concentration of donepezil everywhere outside the inlet segment is zero initially ( $t = 0$  seconds).

### D. Acquisition of Drug-Specific Parameters

To our knowledge, there are no studies that explicitly list the diffusion coefficient of donepezil through any layer of the BBB nor the brain parenchyma. However, Fanizza *et al.* [20] utilized a diffusion coefficient  $D_2 = 7.2772 \times 10^{-12} \text{ m}^2 \text{ s}^{-1}$  for simulating donepezil transport through collagen–polyethylene glycol (COLL–PEG) hydrogel via numerical model. Despite these physiological differences in transport medium, it has been previously justified that the diffusion coefficient of a bioactive molecule within a physiological membrane can be

TABLE II  
FLUID FLOW PARAMETERS USED IN NUMERICAL MODEL

Parameter	Value	Unit	Ref.
Diffusivity of blood in tissue ( $D_1$ )	$0.4 \times 10^{-9}$	$\text{mm}^2 \text{ s}^{-1}$	[8]
Diffusivity of donepezil in tissue ( $D_2$ )	$7.2772 \times 10^{-12} \text{ m}^2 \text{ s}^{-1}$		[20]
Inlet velocity of blood ( $u_{b,\text{in}}$ )	0.38	$\text{mm s}^{-1}$	[21]
Density of blood ( $\rho_b$ )	1060	$\text{kg m}^{-3}$	[22]
Inlet concentration of donepezil ( $c_{\text{in}}$ )	$1.41 \times 10^{-4}$	$\text{mol m}^{-3}$	[23]
Porosity of BBB layers	0.1–0.9		
<b>Carreau blood flow model</b>			
Zero shear rate viscosity ( $\mu_0$ )	0.056	Pas	[17], [24]
Infinite shear rate viscosity ( $\mu_\infty$ )	0.00345	Pas	[17], [24]
Relaxation time ( $\lambda$ )	3.313	s	[17], [24]
Power index ( $n$ )	0.3568		[17], [24]

approximated with their diffusion coefficient within water or organic solvent [25], [26]. Given the fact that the COLL–PEG hydrogel in Fanizza *et al.* [20] included structural protein (collagen) in its medium in addition to organic solvent (PEG), and that there were no other diffusivities for donepezil properly available, the diffusion coefficient  $D_2 = 7.2772 \times 10^{-12} \text{ m}^2 \text{ s}^{-1}$  was deemed acceptable for numerical modeling purposes.

Furthermore, we used the half-maximal inhibitory concentration ( $\text{IC}_{50}$ ) value of donepezil in plasma, given as  $53.6 \text{ ng mL}^{-1}$  [23]. By definition, the  $\text{IC}_{50}$  value is the concentration of donepezil in plasma that inhibits AChE activity by 50% [27]. This raw value was converted to proper units via stoichiometric calculation, using  $379.5 \text{ g mol}^{-1}$  as the molecular weight of donepezil [16]. A value of  $c_{\text{in}} = 1.41 \times 10^{-4} \text{ mol m}^{-3}$  was obtained.

## III. RESULTS AND DISCUSSION

### A. Effect of Porosity on Spatial Concentration Profile

We first examined the effect of porosity of the blood–brain barrier on the concentration profile of donepezil. Since the concentration profile of donepezil is unsteady at short times, a reference time of  $t = 10$  seconds elapsed since the start of the numerical study was established for comparison purposes. Then, a second probe (“centerline”) was added at  $z = 6.2 \mu\text{m}$  to measure the spatial concentration profile of donepezil (fig. 4a).

The results obtained by the parametric sweep show that for any given porosity, the concentration of donepezil decreases

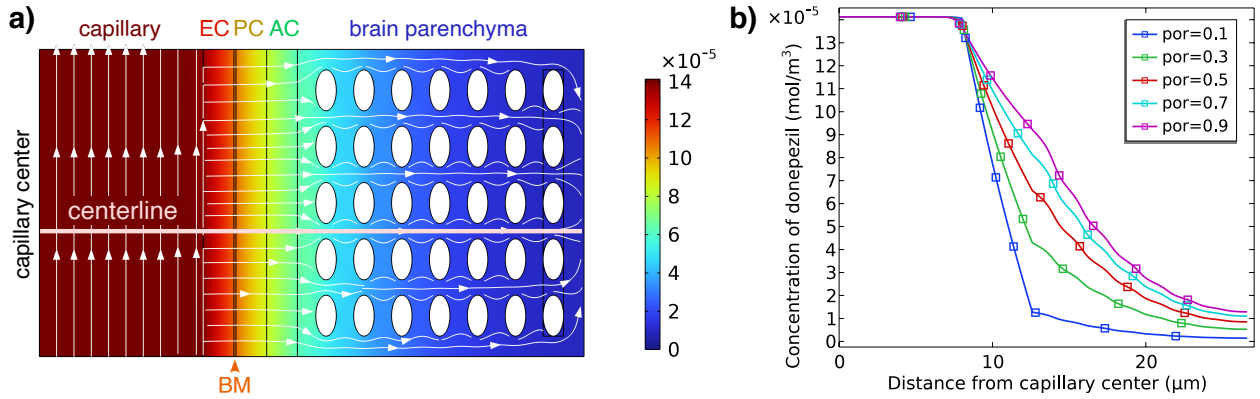


Fig. 4. a) The spatial concentration profile ( $\text{mol m}^{-3}$ ) of donepezil over the numerical BBB model. EC = endothelial cell layer; BM = basement membrane; PC = pericyte layer; AC = astrocyte endfoot. A concentration “centerline” was established at  $z = 6.2 \mu\text{m}$ . The present state of the system is under BBB porosity  $\varepsilon_p = 0.5$  and at time  $t = 10$  seconds. b) The concentration profile of donepezil ( $\text{mol m}^{-3}$ ) measured over the concentration centerline ( $z = 6.2 \mu\text{m}$ ) at  $t = 10$  s plotted under five different porosities ( $\varepsilon_p = 0.1, 0.3, 0.5, 0.7, 0.9$ ). Here, we use por to denote porosity  $\varepsilon_p$  of the BBB.

as the radial position  $r$  from the capillary center ( $r = 0$ ) increases (fig. 4b). We expect that this is due to mass transfer resistance of the various layers of the BBB against donepezil transport. As the issue with drug transport across the BBB suggests, the concentration of donepezil is very low relative to the inlet concentration. At porosity  $\varepsilon_p = 0.1$ , the concentration at the end of the parenchymal region ( $r = R_{\max}$ ) is  $1.792 \times 10^{-6} \text{ mol m}^{-3}$ ; at  $\varepsilon_p = 0.9$ , the concentration is  $1.2385 \times 10^{-5} \text{ mol m}^{-3}$  (fig. 4b). This is in relation with the inlet concentration of  $1.41 \times 10^{-4} \text{ mol m}^{-3}$  (table II).

More importantly, as the porosity of the BBB is increased, the concentration profile of donepezil increases everywhere along the concentration centerline (fig. 4b). As the BBB layers are rendered more porous, the administered donepezil undergoes less mass transfer resistance through the layers.

### B. Effect of Porosity on Drug Delivery Efficacy

Under a fixed porosity value  $\varepsilon_p$  of the BBB, we define the *drug delivery efficacy* at time  $t$  to be

$$\eta(\varepsilon_p, t) = \overline{c_{\text{probe}}}(t) / c_{\text{in}} \quad (13)$$

where  $\overline{c_{\text{probe}}}(t)$  is the average concentration of donepezil measured at the concentration probe at time  $t$ , and  $c_{\text{in}}$  is the concentration of donepezil at the inlet of the capillary domain (as listed in table II).

The numerical model was solved iteratively for five different porosity values ( $\varepsilon_p = 0.1, 0.3, 0.5, 0.7, 0.9$ ) over a simulation period of  $t = 60$  seconds. We found that, with increasing deterioration level and therefore porosity of the BBB, the value of  $\eta|_t$  had increased over the concentration probe for all simulation times  $0 \leq t \leq 60$  seconds (fig. 5).

At  $\varepsilon_p = 0.1$ , the drug delivery efficiency at the probe is approximately  $\eta(t = 60 \text{ s}) \approx 0.164 = 16.4\%$ , which reflects the impenetrability of the BBB under a less deteriorated state. When the porosity is between  $0.5 \leq \varepsilon_p \leq 0.9$ , the efficiency is profoundly amplified compared to that under  $\varepsilon_p = 0.1$ , ranging between 55% and 75%. This corroborates with the porosity effects on the donepezil concentration profile, as displayed in the previous section (fig. 4, section III-A). However, the

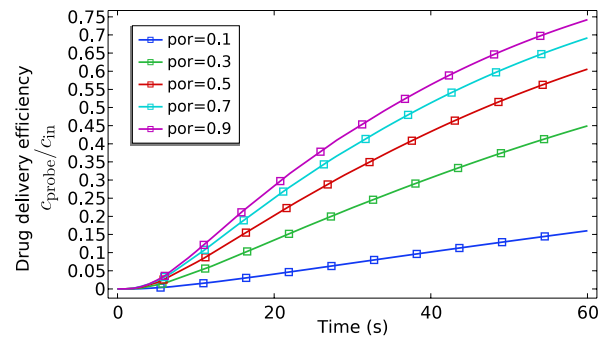


Fig. 5. The drug delivery efficacy  $\eta(\varepsilon_p, t)$  of donepezil transport across the BBB, plotted over the first 60 seconds of simulation time. The  $\eta$ -profile is plotted over different porosities ( $\varepsilon_p = 0.1, 0.3, 0.5, 0.7, 0.9$ , denoted por) of the BBB.

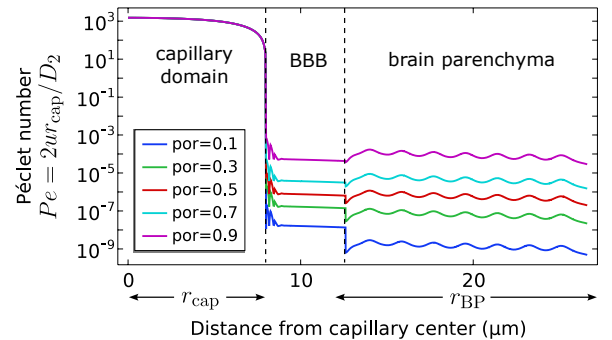


Fig. 6. The Péclet number describing donepezil transport plotted over radial distance from the capillary center ( $\mu\text{m}$ ), under different porosities of the BBB. Note the Péclet number is plotted on a logarithmic scale.

differences in  $\eta$ -profiles are less drastic under higher elapsed times.

### C. Effect of Porosity on Mass Transport Mechanism

Next, the effect of deterioration of the BBB on the mechanism of donepezil transport was investigated. More specifically, we explored the effects of porosity on the Péclet number,

defined as the ratio between transport rate due to advection and transport rate due to diffusion.

$$Pe = \frac{L^2/D}{L/u} = \frac{uL}{D} \quad (14)$$

Here,  $u$  is the magnitude of the velocity field  $\mathbf{u}$ ,  $L$  is the characteristic length, assigned to be the diameter of the capillary domain  $2r_{\text{cap}} = 8 \mu\text{m}$ , and  $D = D_2 = 7.2772 \times 10^{-12} \text{ m}^2 \text{ s}^{-1}$  is the diffusion coefficient of donepezil through tissue.

The results from iteratively solving the Péclet number of substrate transport along the “concentration centerline” (definitively shown in fig. 4a) are shown in fig. 6. It is worthy to mention that the Péclet number profile was shown the same throughout all simulation times.

In the capillary domain, the Péclet number is approximately  $Pe \approx 1500 \gg 1$ ; this suggests that donepezil transport within the capillary is predominately driven by advection. When donepezil reaches the BBB domain starting at  $r = r_{\text{cap}}$ , the Péclet number declines by at least six orders of magnitude (fig. 6). At porosity  $\varepsilon_p = 0.9$ , the Péclet number drastically declines to  $Pe \approx 5.06 \times 10^{-5}$ , whereas at porosity  $\varepsilon_p = 0.1$ , the Péclet number declines to  $Pe \approx 1.60 \times 10^{-8}$ . Since  $Pe \ll 1$ , it can be inferred that the dominating transport mechanism switches to diffusion, due to the mass transfer resistance of the tight junctions. Similarly, drug transport within the brain parenchyma (region marked  $r_{\text{BP}}$ ; see fig. 6) has been shown to have a slightly decreased Péclet number profile compared to the BBB; this implies that drug delivery in the brain parenchyma is primarily diffusion-controlled, like in the BBB.

The observed trend in fig. 6 shows that an increase in porosity of the BBB induces an increase in convective mechanism over diffusive mechanism of donepezil transport. The promotion in convection-driven transport may explain why drug delivery efficiency at the concentration probe is higher when the BBB is in a state of increased deterioration.

#### IV. CONCLUSIONS

In the present paper, we constructed a numerical model of the BBB assuming a simplified, cylindrical, and axisymmetric geometry. Using this model, we ran a sensitivity analysis on this numerical model to examine how the porosity of the BBB affects the transport dynamics of donepezil, an AChE inhibitor and commonly administered AD drug, throughout the barrier, assuming equal porosity in all layers. We obtained the following key results:

- The concentration profile over a linear probe from the capillary center to the brain parenchyma reflects the mass transfer resistance of the BBB layers, as well as the parenchyma.
- Drug delivery efficacy at the concentration probe, situated at the farther end of the brain parenchyma, is greatly amplified under states of increased porosity. For instance, at  $t = 60$  seconds of simulation time, the efficacy increased from 16.4% to 75% at approximately  $13 \mu\text{m}$  away from the capillary wall.
- The predominant mechanism driving drug transport within the capillary domain is convection. Within the

BBB and brain parenchyma, however, this mechanism primarily switches to diffusion. The degree of convection relative to diffusion in both the BBB and parenchyma, however, can be increased with higher porosity states within the BBB.

#### A. Future Steps and Additional Insights

Overall, the study elucidated drug delivery dynamics of donepezil through the BBB at different stages of deterioration, indicative of the severity of AD. However, there is much left to study on optimizing efficacy of donepezil delivery considering the following key parameters:

1) *Toxicity*: While an effective AD symptom reliever, donepezil is known to induce bradycardia, even in patients without underlying cardiac abnormalities. Donepezil is observed to alter the activity of the vagus nerve, leading to these conditions [28]. It is thus worthwhile to study the transport of donepezil through the BBB to the vagus nerve area.

2) *Drug–enzyme interactions*: Donepezil is metabolized in the liver by enzymes including CYP2D6 and CYP3A4. When these enzymes are induced by drugs like phenytoin and carbamazepine, they can break down donepezil more quickly and reduce its concentration in the bloodstream [28]. Understanding how donepezil concentration changes over prolonged periods of time in presence of these drugs can shed light on the long-term transport of donepezil to the desired site.

3) *Lack of experimental data*: The lack of available data on donepezil diffusion forced many assumptions within this study. Furthermore, the mathematical range used for tissue porosity in the study is not a measured range as there lacks studies providing such data. Therefore, studies to rigorously measure the porosity of the BBB layers can greatly improve the modeling of diffusion and fluid flow through the BBB. Discovering more accurate measurements of the diffusive properties of donepezil and the BBB layers via *in vivo* studies can improve the predictive ability of this model as well as future models.

4) *Mechanism of Drug Transport*: The study only reached as far as observing both convective and diffusive mass transport as well as assuming paracellular transport across the BBB. We have modeled carrier-mediated transport [11] as part of porosity but did not expand on this further. An improvement on our model would be to implement active and passive transport of donepezil to gain a better understanding of its transport dynamics.

5) *Personalized Medicine Approach*: The study focused on a 5 mg oral dosage of donepezil, overlooking variations per individual in BBB permeability across different stages of AD [26]. Current research lacks extensive exploration of BBB deterioration and AD progression. Furthermore, the obtainable dosages of donepezil (e.g. 5 mg, 10 mg, 23 mg) should be considered given a patient’s specific  $IC_{50}$  value, which is affected by genetic variability, disease progression, comorbidities, and concomitant medications [23]. Further development of neuroimaging technologies can help enhance the understanding of a patient’s BBB profile along with a tailored dosage of donepezil required to regulate specific acetylcholine levels.

## REFERENCES

- [1] Breijyeh Z, Karaman R. Comprehensive review on Alzheimer's disease: Causes and treatment. *Molecules*. 2020 Dec;25(24):5789.
- [2] Eldufani J, Blaise G. The role of acetylcholinesterase inhibitors such as neostigmine and rivastigmine on chronic pain and cognitive function in aging: A review of recent clinical applications. *Alzheimer's & Dementia: Translational Research & Clinical Interventions*. 2019;5(1):175-83. Available from: <https://alz-journals.onlinelibrary.wiley.com/doi/abs/10.1016/j.trci.2019.03.004>.
- [3] Anand P, Singh B. A review on cholinesterase inhibitors for Alzheimer's disease. *Arch Pharm Res*. 2013 Apr;36(4):375-99. Available from: <https://doi.org/10.1007/s12272-013-0036-3>.
- [4] Sharma K. Cholinesterase inhibitors as Alzheimer's therapeutics (Review). *Mol Med Rep*. 2019 Jun;20(2):1479-87.
- [5] Daneman R, Prat A. The blood-brain barrier. *Cold Spring Harb Perspect Biol*. 2015 Jan;7(1):a020412.
- [6] Wu D, Chen Q, Chen X, Han F, Chen Z, Wang Y. The blood-brain barrier: structure, regulation, and drug delivery. *Signal Transduct Target Ther*. 2023 May;8(1):217.
- [7] Stamatovic SM, Keep RF, Andjelkovic AV. Brain endothelial cell-cell junctions: how to "open" the blood brain barrier. *Curr Neuropharmacol*. 2008 Sep;6(3):179-92.
- [8] Hassanzadehroodbari M, Soltani M, Heydarinasab A, Nakhjiri AT, Hossain MDK, Khiyavi AA. Mathematical modeling and simulation of molecular mass transfer across blood brain barrier in brain capillary. *Journal of Molecular Liquids*. 2020;310:113254. Available from: <https://www.sciencedirect.com/science/article/pii/S0167732219367595>.
- [9] Sarafraz M, Nakhjavani M, Shigdar S, Christo FC, Rolfe B. Modelling of mass transport and distribution of aptamer in blood-brain barrier for tumour therapy and cancer treatment. *European Journal of Pharmaceutics and Biopharmaceutics*. 2022;173:121-31. Available from: <https://www.sciencedirect.com/science/article/pii/S0939641122000522>.
- [10] Marques F, Sousa JC, Sousa N, Palha JA. Blood-brain-barriers in aging and in Alzheimer's disease. *Molecular Neurodegeneration*. 2013 Oct;8(1):38. Available from: <https://doi.org/10.1186/1750-1326-8-38>.
- [11] Kim MH, Maeng HJ, Yu KH, Lee KR, Tsuruo T, Kim DD, et al. Evidence of carrier-mediated transport in the penetration of donepezil into the rat brain. *J Pharm Sci*. 2010 Mar;99(3):1548-66.
- [12] Wong AD, Ye M, Levy AF, Rothstein JD, Bergles DE, Searson PC. The blood-brain barrier: an engineering perspective. *Front Neuroeng*. 2013 Aug;6:7.
- [13] Sá-Pereira I, Brites D, Brito MA. Neurovascular unit: a focus on pericytes. *Molecular Neurobiology*. 2012 Apr;45(2):327-47. Available from: <https://doi.org/10.1007/s12035-012-8244-2>.
- [14] Yurchenco PD. Basement membranes: cell scaffoldings and signaling platforms. *Cold Spring Harb Perspect Biol*. 2011 Feb;3(2).
- [15] Loopuijt LD, Silva Filho Md, Hirt B, Vonthein R, Kremers J. Dendritic thickness: a morphometric parameter to classify mouse retinal ganglion cells. *Braz J Med Biol Res*. 2007 Aug;40(10):1367-82.
- [16] PubChem. Bethesda, editor. Compound summary for CID 3152, donepezil. National Library of Medicine (US), National Center for Biotechnology Information;. Available from: <https://pubchem.ncbi.nlm.nih.gov/compound/Donepezil>.
- [17] Shibeshi SS, Collins WE. The Rheology of Blood Flow in a Branched Arterial System. *Applied Rheology*. 2005;15(6):398-405. Available from: <https://doi.org/10.1515/arth-2005-0020> [cited 2024-05-04].
- [18] Kruczek B. In: Drioli E, Giorno L, editors. Carman-Kozeny Equation. Berlin, Heidelberg: Springer Berlin Heidelberg; 2015. p. 1-3. Available from: [https://doi.org/10.1007/978-3-642-40872-4\\_1995-1](https://doi.org/10.1007/978-3-642-40872-4_1995-1).
- [19] Royer P. Advection-diffusion in porous media with low scale separation: modelling via higher-order asymptotic homogenisation. *Transp Porous Media*. 2019 Jun;128(2):511-51. Available from: <https://doi.org/10.1007/s11242-019-01258-2>.
- [20] Fanizza F, Boeri L, Donnaloja F, Perottoni S, Forloni G, Giordano C, et al. Development of an induced pluripotent stem cell-based liver-on-a-chip assessed with an Alzheimer's disease drug. *ACS Biomater Sci Eng*. 2023 Jul;9(7):4415-30. Available from: <https://doi.org/10.1021/acsbiomaterials.3c00346>.
- [21] Hudetz AG. Blood Flow in the Cerebral Capillary Network: A Review Emphasizing Observations with Intravital Microscopy. *Microcirculation*. 1997;4(2):233-52. Available from: <https://onlinelibrary.wiley.com/doi/abs/10.3109/10739689709146787>.
- [22] Kenner T. The measurement of blood density and its meaning. *Basic Res Cardiol*. 1989 Mar;84(2):111-24. Available from: <https://doi.org/10.1007/BF01907921>.
- [23] Ota T, Shinotoh H, Fukushi K, Kikuchi T, Sato K, Tanaka N, et al. Estimation of plasma IC50 of donepezil for cerebral acetylcholinesterase inhibition in patients with Alzheimer disease using positron emission tomography. *Clin Neuropharmacol*. 2010 Mar;33(2):74-8.
- [24] Johnston BM, Johnston PR, Corney S, Kilpatrick D. Non-Newtonian blood flow in human right coronary arteries: steady state simulations. *J Biomech*. 2004 May;37(5):709-20.
- [25] Lomize AL, Pogozheva ID. Physics-based method for modeling passive membrane permeability and translocation pathways of bioactive molecules. *J Chem Inf Model*. 2019 Jul;59(7):3198-213. Available from: <https://doi.org/10.1021/acs.jcim.9b00224>.
- [26] Bemporad D, Essex JW, Luttmann C. Permeation of small molecules through a lipid bilayer: a computer simulation study. *J Phys Chem B*. 2004 Apr;108(15):4875-84. Available from: <https://doi.org/10.1021/jp035260s>.
- [27] Aykul S, Martinez-Hackert E. Determination of half-maximal inhibitory concentration using biosensor-based protein interaction analysis. *Anal Biochem*. 2016 Jun;508:97-103.
- [28] Kumar A, Gupta V, Sharma S. Donepezil. StatPearls Publishing; 2023. Available from: <https://www.ncbi.nlm.nih.gov/books/NBK513257/>.

## ACKNOWLEDGMENT

The authors would like to thank Professor Aaron Streets, as well as graduate student instructors Javad Aminian-Dehkordi and Erfan Ghazimirsaeed, for providing us the support and feedback necessary to complete this project.

## APPENDICES

Appendices are attached on the following pages.